PRIMITIVE CHONDRULES IN A HIGHLY UNEQUILIBRATED CLAST IN NWA 753 R CHONDRITE

Noriko T. Kita[1], Travis J. Tenner[1], Takayuki Ushikubo[1], Daisuke Nakashima[1], and A. Bischoff [2]

[1]Department of Geoscience, University of Wisconsin-Madison, [2]Institut für Planetologie, Westfälische Wilhelms-Universiät Münster

OBJECTIVES: Understanding the environments and isotope reservoirs of R chondrite forming regions.

Characteristics of R chondrites [1-7]

- FeO-rich olivine (Fa_{38}) in equilibrated lithologies
- High bulk $\Delta^{17}O$ ($=\delta^{17}O-0.52\times\delta^{18}O$) values (~2.7‰)
- A wide range of $\Delta^{17}O$ in chondrules (−4‰ to +3‰)

Oxidized nebula setting with ^{16}O-depleted oxygen isotope reservoirs?

Search for least equilibrated R3 clasts

Most R chondrites are of lower petrologic types (R3 and R4), though unequilibrated R chondrites with subtypes lower than 3.6 are not known. Many R chondrites are regolith breccias containing R3-6 clasts. Unequilibrated R3 clasts (<3.5) have been observed in brecciated R chondrites [4,5].

In order to identify primary oxygen isotope signatures in R chondrite chondrules, we need to search for R3 clasts that experienced minimal parent body metamorphism, equivalent to lowest subtypes (≤3.2).

We performed detailed petrographic descriptions of chondrules in a highly unequilibrated R3 clast from Northwest Africa (NWA) 753 (R3-5) chondrite (Figs. 1,2). The goal of the study is to determine if the clast is suitable for detailed SIMS oxygen isotope analyses.

- NWA 753 "Fragment IX" (8 mm × 4 mm)
- We found 69 chondrules >200 μm in size
- BSE imaging (Hitachi S-3400N SEM)
- SEM-EDX analysis for identification of phases
- Electron Microprobe analyses (Cameca SX51)

Fig. 1. Transmitted light photograph of the clast NWA 753-IX in thin section. The clast (marked by red dashed line) stands out by the dark fine-grained matrix. The scale bar is 1 mm.

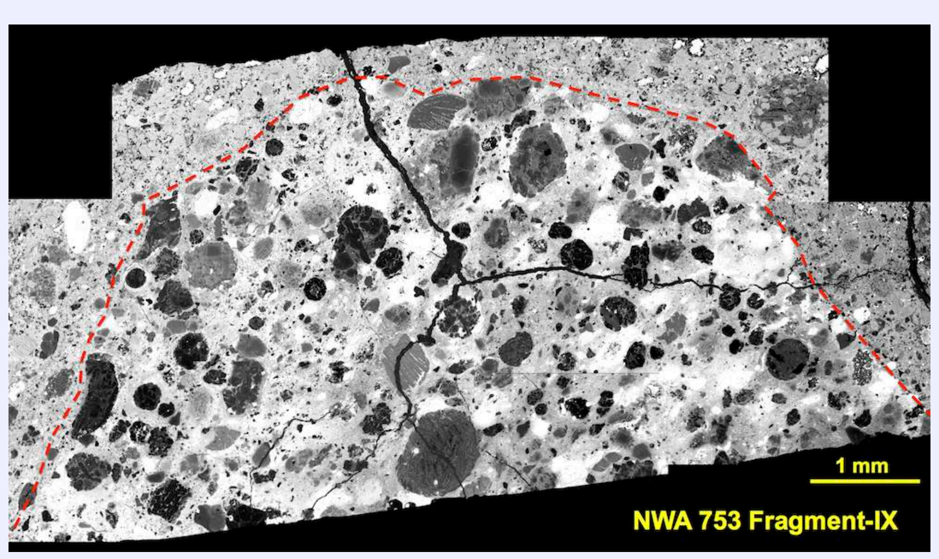

Fig. 2. Backscattered electron image of the clast NWA 753-IX . The clast stands out by the high contrast between chondrules and fine-grained matrix. The scale bar is 1 mm.

Chondrules in R3 clast NWA 753-IX

Most chondrules show porphyritic textures, while minor non-porphyritic chondrules and two Al-rich chondrules [8] are also identified (Table 1, Fig. 3). The proportion of different types of chondrules are very similar to LL3 chondrites [9], especially with respect to similar abundances of type I and II chondrules, while type II chondrules are less abundant in carbonaceous chondrites (~25% in CO3 and ≤5% in CR3 [10-11]). All non-porphyritic chondrules are FeO-rich.

Mesostasis of chondrules are mostly altered compared to unaltered mesostasis seen in type 3.0 chondrites (such as Semarkona [9]) and often include areas with high Na and Cl contents (Fig. 4).

Table 1. Classification of chondrules in NWA 753-IX

Porphyritic (N=59)		Non-porphyritic (N=10)
Al-rich (Al_2O_3>10%) = 2		RP (Radial Pyroxene) = 6
type I (Mg#≥90) [*1]	IA (Ol >80%) = 9 IAB (Ol 20-80%) = 11 IB (Ol<20%) = 9	BO (Barred Olivine) = 3
type II (Mg#<90) [*1]	IIA (Ol >80%) = 20 IIAB (Ol 20-80%) = 7 IIB (Ol<20%) = 1	CC (Crypto-crystalline)= 1

[*1]Mg#: Molar % of [MgO]/[MgO+FeO]

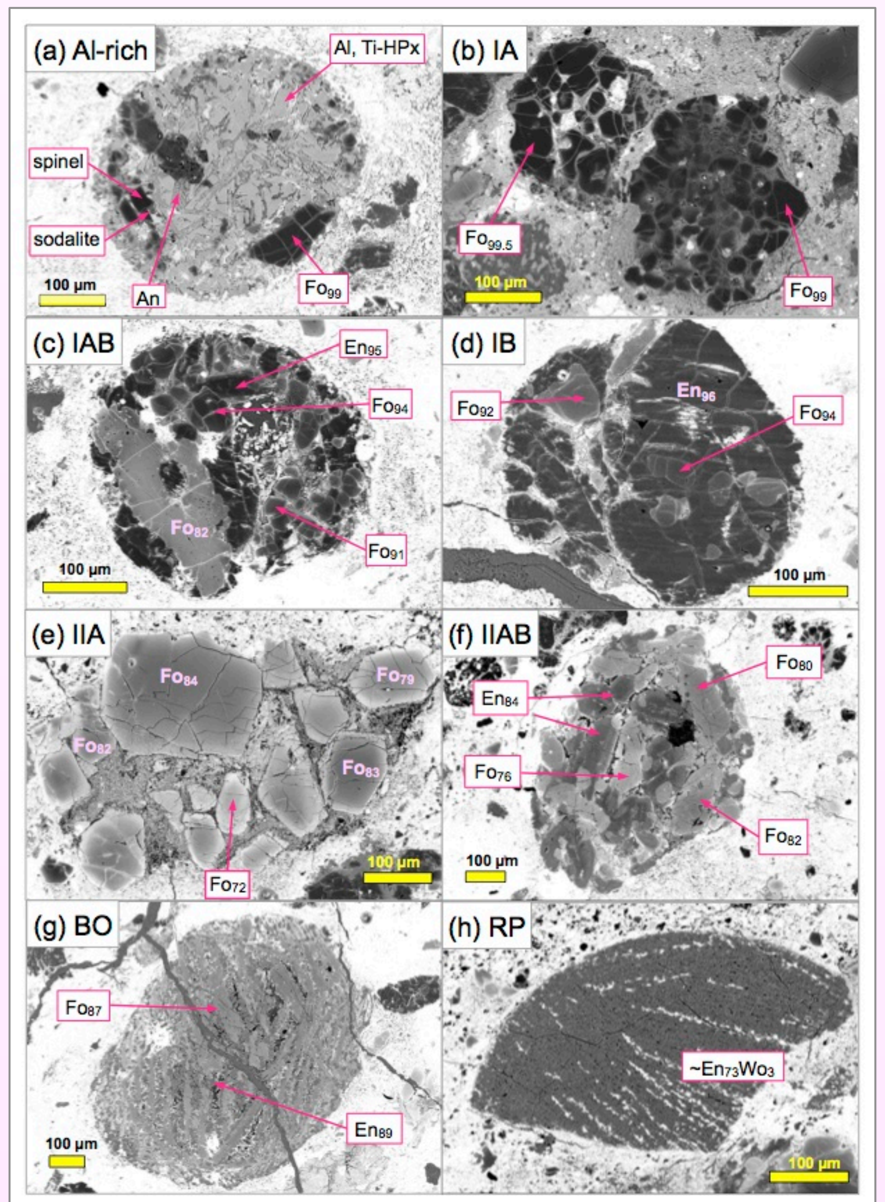

Fig. 3. Major types of chondrules in the R3 clast IX. (a) An Al-rich chondrule, which contains Al-Ti-rich high Ca-pyroxene, and anorthite. (b-f) Ferromagnesian porphyritic chondrules. (g) An FeO-rich barred olivine chondrule. (h) A fragment of radial pyroxene chondrule.

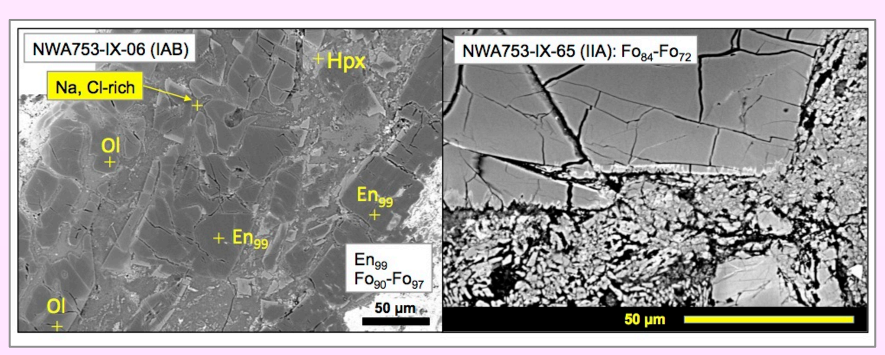

Fig. 4. Alteration textures in the mesostasis of porphyritic chondrules in clast NWA 753-IX. (a) type IAB, (b) type IIA.

Distribution of Chondrule Mg#

The FeO contents of olivine and pyroxene phenocrysts are related to the oxygen fugacity of the chondrule-forming environments [12]. The distribution of Mg# of chondrules in the R3 clast (Fig. 5) is similar to that of LL3, in contrast to carbonaceous chondrites with abundant highly reduced chondrules (Mg#>95). These data indicate that many chondrules in both ordinary chondrite and R chondrite regions formed under more oxidized conditions.

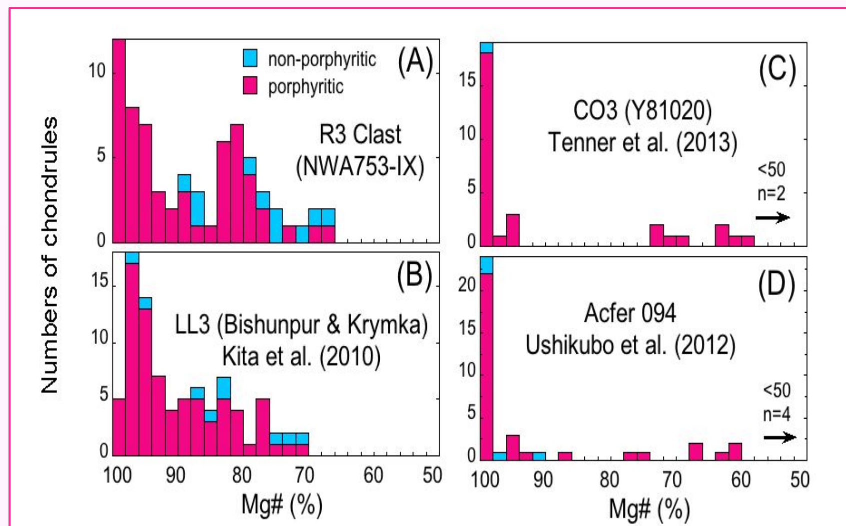

Fig. 5. Histograms of chondrule Mg# in (A) R3 clast NWA 753 IX (this work), (B) LL3 chondrites [9], (C) CO3 [13], and (D) Acfer 094 [14]. The average Mg# of olivine and low-Ca pyroxene phenocrysts were calculated for each chondrule. The Mg# of RP and CC chondrules were also estimated from the average of multiple electron microprobe analyses.

Mineral Chemistry

Most Mg-rich olivine (Mg#>98) in porphyritic chondrules show enrichments of Al_2O_3 and CaO and depletion of MnO when compared to other olivine grains (Fig. 6a-c). This indicates that some type I chondrules in R3 are significantly enriched in refractory elements. They could be related to refractory forsterite grains or forsteritic olivine with ^{16}O-rich isotope signatures that were reported previously from R3 chondrites [7,15]. The average Cr_2O_3 content of ferroan olivine (Fo<98) is 0.17% with a standard deviation (SD) of 0.11% (Fig. 6d). The average value is much lower than that of Semarkona (LL3.0; 0.50±0.10% [16]).

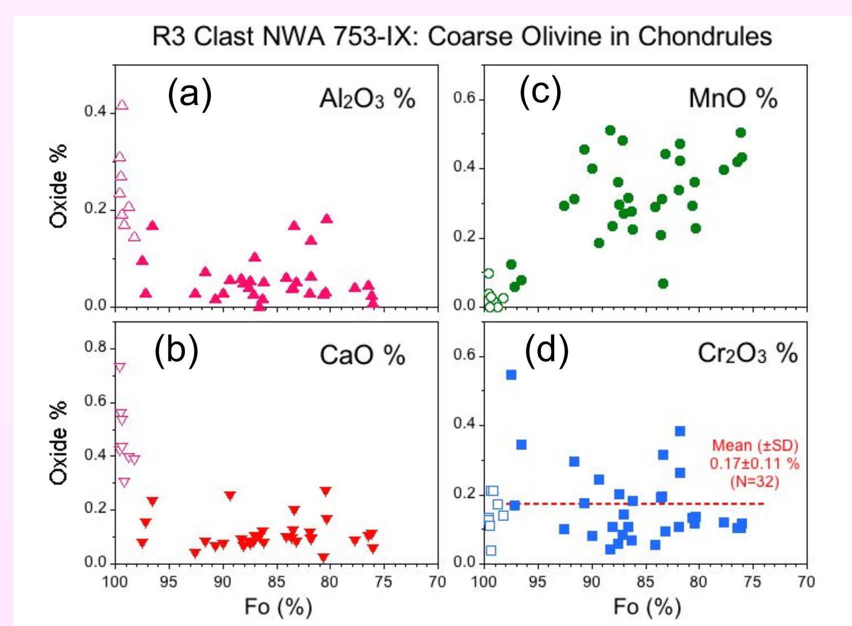

Fig. 6. Minor elements in coarse-grained (≥100 μm) olivine from porphyritic chondrules in NWA 753 IX. Mg-rich olivines (Fo>98) are shown as open symbols. The detection limits of Al_2O_3, CaO, MnO, and Cr_2O_3 are 0.04%, 0.03%, 0.09%, and 0.07%, respectively.

Petrologic Subtypes

Grossman and Brearley [16] suggested that the average and SD of Cr_2O_3 wt% in ferroan olivine grains can be used as an index of low petrologic subtypes from 3.00 to 3.15. The data estimated for the R3 clast NWA 753-IX plot close to the subtypes 3.15-3.20 for ordinary chondrites (Fig. 7). By assuming the classification scheme for ordinary chondrites can be also applied to R chondrites the data suggest that clast NWA 753-IX is the least metamorphosed R3 chondritic material compared to other R3 chondrites (≥3.6).

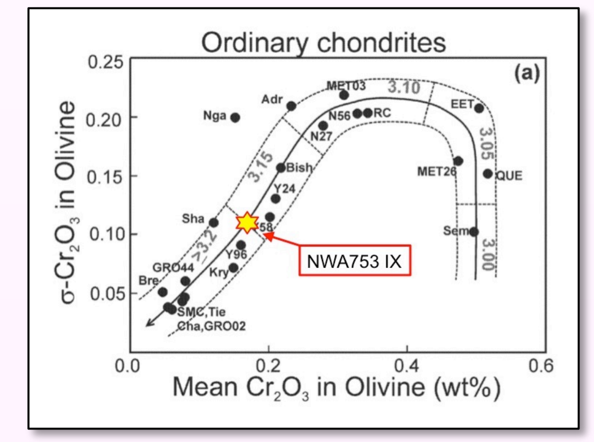

Fig. 7. The average and SD of Cr_2O_3 wt% in olivine (Fo<98) in chondrules from clast NWA 753-IX (Fig. 6d), superimposed on the diagram published by [16].

Future Work: Oxygen isotope Analysis

Group-specific Mg#-$\Delta^{17}O$ trends: High precision SIMS oxygen isotope studies of chondrules in least equilibrated chondrites (Fig, 8; LL, CO, CR, and Acfer 094 with subtypes ≤3.2) revealed group-specific trends between the Mg# and $\Delta^{17}O$ values of chondrules [e.g., 9, 11, 13-14]. These results provide important clues to identify the variety of isotope reservoirs and their evolution in each chondrule forming region.

Both high and low $\Delta^{17}O$ values (+2.7‰ and −4.0‰) from Mg-rich chondrules (Mg#≥99) have been reported for chondrules in R3.6 [7], which are important in understanding the origin of ^{16}O-poor isotope reservoirs in the solar nebula.

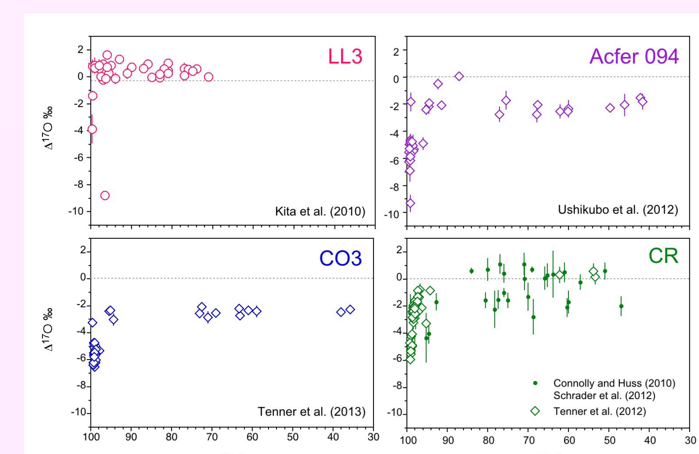

R3 Data ??

Fig. 8. Relationship between Mg# and $\Delta^{17}O$ values of chondrules for individual chondrite groups. Data are from [9, 11, 13-14, 17-18].

SUMMARY

-Highly unequilibrated R3 clast NWA 753-IX contains a variety of chondrules with Mg#'s of 100-67.

-The petrologic subtype is estimated to be 3.15-3.2, suitable for detailed oxygen isotope study.

-More R3 clasts need to be examined.

References: [1] Weisberg M. K. (1991) *GCA, 55,* 2657-2669. [2] Bischoff A. et al. (1994) *Meteoritics, 29,* 264-274. [3] Schulze H. et al. (1994) *Meteoritics, 29,* 275-286. [4] Bischoff A. et al. (2011) *Chemie der Erde, 71,* 101–133. [5] Bischoff A. (2000) *Meteoritics & Planet. Sci., 35,* 699-706. [6] Greenwood J. P. (2000) *GCA, 64,* 3897-3911. [7] Isa J. (2011) *LPS XLII,* Abstract #2623. [8] Bischoff A. and Keil K. (1984) *GCA* 48, 693-709. [9] Kita N. T. et al. (2010) *GCA, 74,* 6610-6635. [10] Kunihiro T. et al. (2005) *GCA, 69* 3831-3840. [11] Tenner T. J. et al. (2012) *LPS XLIII*, Abstract #2127. [12] Ebel D. S. and Grossman L. (2000) *GCA,* 64, 339-366. [13] Tenner T. J. et al. (2013) *GCA, 102,* 226-245. [14] Ushikubo T. (2012) *GCA, 90,* 242-264. [15] Pack A. et al. (2004) *GCA, 68,* 1135-1157. [16] Grossman J. N. and Brearley A. J. (2005) *Meteoritics & Planet. Sci., 40,* 87-122. [17] Connolly H. C. and Huss G. R. (2010) *GCA,* 74, 2473–2483. [18] Schrader D. L. et al. (2012) *GCA,* 101, 302–327.